Report No. NADC-91059-60

THERMAL FATIGUE ANALYSIS OF METAL MATRIX COMPOSITE WITH SPHERICAL REINFORCEMENTS

Eun U. Lee
Air Vehicle and Crew Systems Technology Department (Code 6063)
NAVAL AIR DEVELOPMENT CENTER
Warminster, PA 18974-5000

1 OCTOBER 1991

FINAL REPORT

Approved for Public Release; Distribution is Unlimited

Prepared for
Air Vehicle and Crew Systems Technology Department (Code 606)
NAVAL AIR DEVELOPMENT CENTER
Warminster, PA 18974-5000

NOTICES

REPORT NUMBERING SYSTEM — The numbering of technical project reports issued by the Naval Air Development Center is arranged for specific identification purposes. Each number consists of the Center acronym, the calendar year in which the number was assigned, the sequence number of the report within the specific calendar year, and the official 2-digit correspondence code of the Command Officer or the Functional Department responsible for the report. For example: Report No. NADC-88020-60 indicates the twentieth Center report for the year 1988 and prepared by the Air Vehicle and Crew Systems Technology Department. The numerical codes are as follows:

CODE	OFFICE OR DEPARTMENT
00	Commander, Naval Air Development Center
01	Technical Director, Naval Air Development Center
05	Computer Department
10	AntiSubmarine Warfare Systems Department
20	Tactical Air Systems Department
30	Warfare Systems Analysis Department
40	Communication Navigation Technology Department
50	Mission Avionics Technology Department
60	Air Vehicle & Crew Systems Technology Department
70	Systems & Software Technology Department
80	Engineering Support Group
90	Test & Evaluation Group

PRODUCT ENDORSEMENT — The discussion or instructions concerning commercial products herein do not constitute an endorsement by the Government nor do they convey or imply the license or right to use such products.

Reviewed By: J. Waldman Date: 9 March 92
Branch Head

Reviewed By: [signature] Date: 10 Mar 92
Division Head

Reviewed By: [signature] Date: 16 Mar 92
Director/Deputy Director

REPORT DOCUMENTATION PAGE

Form Approved
OMB No. 0704-0188

1. AGENCY USE ONLY (Leave blank)	2. REPORT DATE	3. REPORT TYPE AND DATES COVERED
	1 October 1991	Final

4. TITLE AND SUBTITLE
Thermal Fatigue Analysis of Metal Matrix Composite with Spherical Reinforcements

5. FUNDING NUMBERS

6. AUTHOR(S)
Eun U. Lee

7. PERFORMING ORGANIZATION NAME(S) AND ADDRESS(ES)
Air Vehicle and Crew Systems Technology Department
(Code 6063)
NAVAL AIR DEVELOPMENT CENTER
Warminster, PA 18974-5000

8. PERFORMING ORGANIZATION REPORT NUMBER
NADC-91059-60

9. SPONSORING/MONITORING AGENCY NAME(S) AND ADDRESS(ES)
Air Vehicle and Crew Systems Technology Department
(Code 606)
NAVAL AIR DEVELOPMENT CENTER
Warminster, PA 18974-5000

10. SPONSORING/MONITORING AGENCY REPORT NUMBER

11. SUPPLEMENTARY NOTES

12a. DISTRIBUTION/AVAILABILITY STATEMENT
Approved for Public Release; Distribution is Unlimited.

12b. DISTRIBUTION CODE

13. ABSTRACT *(Maximum 200 words)*

The stresses and strains, induced by coefficient of thermal expansion (CTE) mismatch, are analyzed for a metal matrix composite with a spherical reinforcement particle. The spherical reinforcement particle is found to be in a hydrostatic stress state and remains in the elastic state. The stresses and strains are largest, and plastic deformation occurs in the matrix adjacent to the reinforcement particle. Accordingly, the reinforcement particle/matrix interface becomes a potential crack initiation site under thermal cycling. The critical internal pressure for plastic deformation is less than 2/3 of the yield stress of the matrix material and it decreases with increasing range of thermal cycle. From the analytically determined strains, the thermal fatigue life can be estimated.

14. SUBJECT TERMS
thermal expansion, stress, strain, metal matrix composite, spherical reinforcement particle, hydrostatic stress, fatigue

15. NUMBER OF PAGES

16. PRICE CODE

17. SECURITY CLASSIFICATION OF REPORT	18. SECURITY CLASSIFICATION OF THIS PAGE	19. SECURITY CLASSIFICATION OF ABSTRACT	20. LIMITATION OF ABSTRACT
Unclassified	Unclassified	Unclassified	SAR

CONTENTS

FIGURES

SYMBOLS

R : radius of matrix hole and reinforcement particle at high temperatures

a : radius of matrix hole after cooling

r_o : radius of reinforcement particle after cooling

r_f : final or effective radius of reinforcement particle under constraint of matrix

r : radial distance

r_d : radius of plastic zone

α : coefficient of thermal expansion (CTE)

α_m : CTE of matrix

α_p : CTE of reinforcement particle

$\Delta\alpha$: $\alpha_m - \alpha_p$ (difference in CTE)

β : constraint factor

δ : misfit factor

ΔT : range of temperature fall

u : radial displacement

u_m : radial displacement in matrix

u_p : radial displacement in reinforcement particle

ν : Poisson's ratio

ν_m : Poisson's ratio of matrix

ν_p : Poisson's ratio of reinforcement particle

E : elastic modulus

E_m : elastic modulus of matrix

E_p : elastic modulus of reinforcement particle

G_m : shear modulus of matrix

B_m : bulk modulus of matrix

SYMBOLS (continued)

p : internal pressure

p_c : critical internal pressure

σ_r : radial stress

$\sigma_\theta, \sigma_\phi$: tangential stresses

$(\sigma_r)_m$: radial stress in matrix

$(\sigma_\theta)_m$, $(\sigma_\phi)_m$: tangential stresses in matrix

$(\sigma_r)_p$: radial stress in reinforcement particle

$(\sigma_\theta)_p, (\sigma_\phi)_p$: tangential stresses in reinforcement particle

$(\sigma_e)_m$: equivalent stress in matrix

$(\sigma_y)_m$: yield stress of matrix

σ_u : ultimate strength

ϵ_r : radial strain

ϵ_θ, ϵ_ϕ : tangential strains

$(\epsilon_r)_m$: radial strain in matrix

$(\epsilon_\theta)_m$, $(\epsilon_\phi)_m$: tangential strains in matrix

$(\epsilon_r)_p$: radial strains in reinforcement particle

$(\epsilon_\theta)_p$, $(\epsilon_\phi)_p$: tangential strains in reinforcement particle

$(\epsilon_r)_m^e$: radial elastic strain component in matrix

$(\epsilon_\theta)_m^e$: tangential elastic strain component in matrix

$(\epsilon_r)_m^p$: radial plastic strain component in matrix

$(\epsilon_\theta)_m^p$: tangential plastic strain component in matrix

$(\epsilon)^e$: elastic strain per thermal cycle

$(\epsilon)^p$: plastic strain per thermal cycle

(ϵ) : total strain per thermal cycle [$= (\epsilon)^e + (\epsilon)^p$]

(ϵ_f) : true fracture strain in a monotonic tensile test

SYMBOLS (continued)

M, z : material constants

N_f : number of thermal cycles at failure

ACKNOWLEDGMENT

This study was supported by the NADC Independent Research Program. The author is grateful to Drs. J. Waldman and W. Scott for their constant encouragement and to Dr. H. Tsai for technical discussion.

INTRODUCTION

Metal matrix composites (MMCs), because of their favorable elevated temperature properties, will be used as structure materials in future aircraft. However, at elevated temperatures, these composites lose some of their room temperature properties. Moreover, the loss becomes much worse and results in material deterioration under thermal cycling.

Thermal fatigue has been reported to occur in various MMCs: tungsten fiber/copper (1,2), tungsten fiber/supperalloys (3), boron fiber/aluminum (4-6), Al_2O_3 (FP) fiber/aluminum (7), FP fiber/magnesium (8), SiC fiber/titanium (9), SiC whisker/aluminum (10), and graphite fiber/aluminum (11) composites. Thermal fatigue is caused by stresses and strains due to repeating constraints of free thermal expansion and contraction. The constraints can be grouped into two categories: external and internal. The external constraint is due to boundary forces applied to the surface of the component which is being heated or cooled. The internal constraint is produced by the difference in coefficients of thermal expansion (CTE) of the constituent phases in the component material: CTE mismatch, and/or non-uniform temperature distribution in the component: thermal gradient. CTE mismatch-induced thermal fatigue is a characteristic with MMCs, since this mismatch for most of MMCs is large.

The Coffin-Manson relationship for low cycle fatigue (12,13) is reported to be applicable for thermal fatigue (13,14). Therefore, the thermal strains, elastic and plastic, generated by the CTE mismatch, are essential in the analysis of thermal fatigue of MMCs. Thermal stress and strain have been analyzed extensively for continuous fiber (15-31) and whisker reinforced (32, 33) MMCs. However, such analysis has been very limited for particulate MMC (34, 35).

This report presents the analysis of thermal stresses and strains, caused by CTE mismatch between the spherical reinforcement particle and the matrix in an MMC, and the estimation of the thermal fatigue life. In the analysis, the following assumptions are used.

1. The reinforcement particle is a sphere in an infinite matrix of an MMC.

2. The matrix has elastic-perfectly plastic behavior.

3. The stress-strain behavior is independent of strain rate and stress orientation.

4. The temperature in the MMC is uniform at all time. Therefore, there is no thermal gradient in the MMC.

STRESS AND STRAIN ANALYSIS

The thermal stresses and strains, induced by CTE mismatch, will be analyzed under purely elastic conditions first and then under plastic conditions.

A. Thermoelastic Stresses and Strains

The following elastic model was used in the analysis of thermoelastic stresses and strains.

1. At high temperatures, the radii of the matrix hole and the reinforcement particle are identical R, (Figure 1).

2. Upon cooling, the matrix hole tries to contract to a, and the reinforcement particle, with a lower CTE, tries to contract only to r_0, (Figure 1).

3. The final or effective radius of the reinforcement particle under the constraint of the matrix is r_1, (Figure 1).

The radii and their relationship can be denoted by the following equations.

$$a = R(1 - \alpha_m \Delta T) \quad (1)$$

$$r_0 = R(1 - \alpha_p \Delta T) = a(1 + \delta) \quad (2)$$

$$r_1 = a(1 + \beta\delta) \quad (3)$$

where

α_m : CTE of matrix

α_p : CTE of reinforcement particle

δ : misfit factor

β : constraint factor

ΔT : range of temperature fall

$\Delta\alpha$: $\alpha_m - \alpha_p$

From Equations (1) and (2), the misfit factor δ can be described as a function of difference in CTEs, range of temperature fall ΔT, and CTE of matrix α_m, Equation (4).

$$\delta = \Delta\alpha / [\,(1/\Delta T) - \alpha_m\,] \quad (4)$$

Throughout this analysis, spherical coordinates are used. The origin is located at the center of the spherical reinforcement particle. Because of symmetry, the tangential displacement as well as the shear stress and strain are all zero, and the radial displacement u is a function of radial distance r. There are three non-zero stress components, a radial stress σ_r and two tangential stresses σ_θ and σ_ϕ. These stresses must satisfy the equilibrium condition in the radial direction, Equation (5).

$$d\sigma_r/dr + (2/r) \cdot (\sigma_r - \sigma_\theta) = 0 \tag{5}$$

Furthermore,

$$\sigma_\theta = \sigma_\phi \text{ and } \epsilon_\theta = \epsilon_\phi \tag{6}$$

In a cooled body, the total strain is made up of two components in each of the radial and tangential directions, Equations (7) and (8). One component is a uniform contraction proportional to the range of temperature fall. Since this contraction is equal in all directions, only normal strains and no shear strains are found. Thus, the normal contraction in any direction is $-\alpha\Delta T$. The other component comprises the strains required to maintain the continuity of the body. These strains are related to the stresses by means of Hooke's law of isothermal elasticity.

$$\epsilon_r = (1/E) \cdot (\sigma_r - 2\nu\sigma_\theta) - \alpha\Delta T \tag{7}$$

$$\epsilon_\theta = (1/E) \cdot [-\nu\sigma_r + (1 - \nu)\sigma_\theta] - \alpha\Delta T \tag{8}$$

Furthermore, the radial and tangential strain components are defined as

$$\epsilon_r = du/dr, \quad \epsilon_\theta = u/r \tag{9}$$

where

r : radial distance

σ_r, ϵ_r : radial stress and strain

σ_θ, σ_ϕ, : ϵ_θ, ϵ_ϕ : tangential stresses and strains

u : radial displacement

ν : Poisson's ratio

E : elastic modulus

α : CTE

From Equation (5) and Equations (7) - (9), the equilibrium equation can be expressed with radial displacement u and distance r.

$$d^2u/dr^2 + (2/r) \cdot (du/dr) - 2u/r^2 = 0 \tag{10}$$

The general solution of Equation (10) is:

$$u = C_1 r + C_2/r^2 \tag{11}$$

The boundary condition for the matrix is

$$(u_m)_{r=r_1} = r_1 = a = a\beta\delta, \ (u_m)_{r=\infty} = 0 \tag{12}$$

where u_m is the radial displacement in the matrix.

Then,

$$\begin{gathered} C_1 = 0, \ C_2 = a^3\beta\delta \ (1+\beta\delta) \\ (u_m)_{r>r_1} = a^3\beta\delta \ (1 + \beta\delta) \ / \ r^2 \end{gathered} \tag{13}$$

The boundary condition for the spherical reinforcement particle is

$$(u_p)_{r=r_1} = r_1 = r_o = a(\beta - 1)\delta, \ (u_p)_{r=o} = 0$$

where u_p is the radial displacement in the spherical reinforcement particle.

Then,

$$C_1 = (\beta - 1)\delta / (1 + \beta\delta),\ C_2 = 0$$
$$(u_p)_{r < r_1} = (\beta - 1)\delta r / (1 + \beta\delta) \tag{14}$$

Substituting this value of u_p into Equation (9) gives the elastic strains within the reinforcement particle.

$$(e_r)_p = (e_\theta)_p = (\beta - 1)\delta / (1 + \beta\delta) \tag{15}$$

From Equations (6) - (8) and Equation (15), the elastic stress components within the reinforcement particle are determined to be

$$(\sigma_r)_p = (\sigma_\theta)_p = (\sigma_\phi)_p$$
$$= [\ E_p/(1 - 2\nu_p)\ ] \cdot [\ (\beta - 1)\delta / (1 + \beta\delta) + \alpha_p \Delta T\ ] \tag{16}$$

This equation indicates that the spherical reinforcement particle is in a state of hydrostatic stress, which is larger with larger elastic modulus, CTE, and temperature range. Consequently, the reinforcement particle is in an elastic state and it is not plastically deformed.

Substituting the displacement value in the matrix, Equation (13), into Equation (9) furnishes the elastic strain components in the matrix as follows.

$$(e_r)_m = -2\,(e_\theta)_m = -2\beta\delta(1 + \beta\delta) \cdot (a/r)^3$$
$$= -\lambda(r_1 / r)^3 \tag{17}$$

where

$$\lambda = 2\beta\delta(1 + \beta\delta)^2$$

The feature of elastic strain component variation with radial distance in the matrix is shown in a plot of elastic strain component, normalized with λ, vs. radial distance r, Figure 2. The magnitude of each elastic strain component is largest at the reinforcement particle/matrix interface, $r = r_1$, and decreases with increasing distance from the interface.

From Equations (7), (8) and (17), elastic stress components in the matrix are found to be

$$(\sigma_r)_m = -[\, 2E_m\beta\delta(1+\beta\delta) / (1 + \nu_m)\,] \cdot (a/r)^3 + (E_m\alpha_m\Delta T) / (1 - 2\nu_m) \\ = -2G_m\lambda(r_1/r)^3 + 3B_m\alpha_m\Delta T \qquad (18)$$

$$(\sigma_\theta)_m = [\, E_m\beta\delta(1 + \beta\delta)/(1 + \nu_m)\,] \cdot (a/r)^3 + (E_m\alpha_m\Delta T) / (1 - 2\nu_m) \\ = G_m\lambda(r_1/r)^3 + 3B_m\alpha_m\Delta T \qquad (19)$$

where

G_m : shear modulus of matrix

B_m : bulk modulus of matrix

The features of the elastic stress component variation with radial distance in the matrix is shown in a plot of $[\, (\sigma_r)_m - 3B_m\alpha_m\Delta T\,] / G_m\lambda$ vs. r and $[\, (\sigma_\theta)_m - 3B_m\alpha_m\Delta T\,] / G_m\lambda$ vs. r, Figure 3. The magnitude of each elastic stress component is also largest at the reinforcement particle/matrix interface, $r = r_1$, and decreases with increasing distance from the interface.

B. Plastic Deformation

As was pointed out, the spherical reinforcement particle remains in an elastic state and the stresses are greatest in the matrix adjacent to the reinforcement particle. For the analysis of plastic deformation, the following model is taken.

1. A thick hollow sphere is deformed, elastically and plastically, under uniformly distributed internal pressure, Figure 4.

2. The internal pressure is produced by a misfitting spherical reinforcement particle.

The internal pressure ρ is identified as the radial stress component at the reinforcement particle/matrix interface, $r = r_1$. Thus from Equation (18),

$$\rho = -(\sigma_r)_m = -[\{2E_m\beta\delta(1+\beta\delta)\}/(1+\nu_m)]\cdot(a/r_1)^3 + (E_m\alpha_m\Delta T)/(1-2\nu_m) = -2G_m\lambda + 3B_m\alpha_m\Delta T \quad (20)$$

According to the von Mises yield criterion (36), plastic deformation occurs if an equivalent stress $(\sigma_e)_m$, defined by the following formula, reaches the yield stress of the matrix $(\sigma_y)_m$.

$$(\sigma_e)_m = (1/\sqrt{2})\cdot[\{(\sigma_r)_m - (\sigma_\theta)_m\}^2 + \{(\sigma_\theta)_m - (\sigma_\phi)_m\}^2 + \{(\sigma_\phi)_m - (\sigma_r)_m\}^2]^{1/2} \quad (21)$$

Since

$$(\sigma_\theta)_m = (\sigma_\phi)_m, \quad (\sigma_e)_m = (\sigma_\theta)_m - (\sigma_r)_m \quad (22)$$

From Equation (19) with $r = r_1$, Equation (20), and the above equation, plastic deformation starts at the reinforcement particle/matrix interface, if the following condition is satisfied.

$$(\sigma_\theta)_m = -(3/2)\,[\rho_c - (E_m\alpha_m\Delta T)/(1-2\nu_m)] = (\sigma_y)_m \qquad (23)$$

where ρ_c is the critical internal pressure for plastic deformation (or yielding) of the matrix.

From Equation (23),

$$\rho_c = -[\,(2/3)(\sigma_y)_m - (E_m\alpha_m\Delta T)\,/\,(1-2\nu_m)\,] \qquad (24)$$

This equation indicates that:

1. The critical internal pressure for plastic deformation is less than 2/3 of the yield strength of a given matrix material.

2. Its magnitude decreases linearly with increasing range of temperature fall and decreasing yield strength.

3. Its magnitude is reduced further for any other matrix material with larger elastic modulus and CTE.

With increasing internal pressure beyond the critical value ρ_c, a plastic zone is formed in the immediate vicinity of the reinforcement particle/matrix interface and extended to a certain radius r_d. This radius r_d separates the inner plastic zone from the outer elastic zone. The equilibrium equation for the plastic zone is obtained by substituting the yield condition

$$(\sigma_e)_m = (\sigma_y)_m - (\sigma_\theta)_m - (\sigma_r)_m$$

into Equation (5). The equilibrium equation is

$$d(\sigma_r)_m/dr - 2(\sigma_y)_m/r = 0 \tag{25}$$

Integrating Equation (25),

$$(\sigma_r)_m = 2(\sigma_y)_m \cdot \ln r + C \tag{26}$$

Using the boundary condition $(\sigma_r)_m = -\rho$ at $r = r_1$, the constant C becomes

$$C = -\rho - 2(\sigma_y)_m \cdot \ln r_1 \tag{27}$$

From Equations (25) - (27), the stress components in the plastic zone, $(r_1 \le r \le r_d)$, are

$$(\sigma_r)_m = 2(\sigma_y)_m \cdot \ln(r/r_1) - \rho \tag{28}$$

$$(\sigma_\theta)_m = (\sigma_y)_m \cdot [\, 2 \cdot \ln(r/r_1) + 1] - \rho \tag{29}$$

The stress components in the elastic zone, $(r_d \le r)$, can he found by substituting ρ_c for ρ and r_d for r_1 in Equations (28) and (29) as follows.

$$(\sigma_r)_m = (\sigma_y)_m [\, (2/3) + 2 \cdot \ln(r/r_d) \,] - (E_m \alpha_m \Delta T)/(1 - 2\nu_m) \tag{30}$$

$$(\sigma_\theta)_m = (\sigma_y)_m [(3/5) + 2 \cdot \ln(r/r_d)] - (E_m \alpha_m \Delta T)/(1-2\nu_m) \quad (31)$$

At the boundary, which separates the plastic and elastic zones, the radial stress components are identical, i.e., Equation (28) = Equation (30) at $r = r_d$. From this relationship, the plastic zone radius r_d is determined as

$$r_d = r_i \cdot \exp[(5/6) + \{ 1/(2 (\sigma_y)_m) \} \cdot \{ p - (E_m \alpha_m \Delta T)/(1-2\nu_m) \}] \quad (32)$$

By substituting $(\sigma_r)_m$ of Equation (30) and $(\sigma_\theta)_m$ of Equation (31) into the equations of stress-strain relation, Equations (7) and (8), the radial and tangential strain components, $(\epsilon_r)_m$ and $(\epsilon_\theta)_m$, in the elastic zone of the matrix is found as

$$(\epsilon_r)_m = (\sigma_y)_m/E_m) \cdot [(2/3) \cdot (1-5\nu_m) + (1-2\nu_m) \cdot \ln(r/r_d)^2] - 2\alpha_m \Delta T \quad (33)$$

$$(e_\theta)_m = (\sigma_y)_m/E_m) \cdot [(1/3) \cdot (5-7\nu_m) + (1-2\nu_m) \cdot \ln(r/r_d)^2] - 2\alpha_m \Delta T \quad (34)$$

In the plastic zone, the stress-strain relations are described as

$$(e_r)_m = du/dr = (1/E_m) \cdot [(\sigma_r)_m - 2\nu_m (\sigma_\theta)_m] - \alpha_m \Delta T + (e_r)_m^p \quad (35)$$

$$(e_\theta)_m = u/r = (1/E_m) \cdot [-\nu_m (\sigma_r)_m + (1-\nu_m) \cdot (\sigma_\theta)_m] - \alpha_m \Delta T + (e_\theta)_m^p \quad (36)$$

where $(\epsilon_r)_m^P$ and $(\epsilon_\theta)_m^P$ are plastic strain components in radial and tangential directions, respectively. From the incompressibility condition for plastic strains, $(\epsilon_r)_m^P + 2(\epsilon_\theta)_m^P = 0$, and Equations (35) and (36), the following differential equation is derived.

$$du/dr + 2u/r - (1/B_m)\,[\,2(\sigma_y)_m \cdot \ln(r/r_1) + \{\,2(\sigma_y)_m - 3\rho\,\}/3\,] - 3\alpha_m \Delta T \qquad (37)$$

where $B_m = E_m/3(1 - 2\nu_m)$ is the bulk modulus of the matrix. Its general solution is

$$u = 2(\sigma_y)_m \cdot r \cdot \ln(r/r_1)/3B_m - \rho r/3B_m - \alpha_m \cdot r \cdot \Delta T + C/r^2 \qquad (38)$$

The constant C is calculated from the displacement at the plastic-elastic zone boundary u, given by Equation (34), for $r = r_d$ as follows:

$$C = (\sigma_y)_m \cdot r_d^3 \nu_m / E_m \qquad (39)$$

From Equations (38) and (39), the displacement in the plastic zone ($r_1 \le r \le r_d$) u can be written as

$$u = 2(\sigma_y)_m \cdot r \cdot \ln(r/r_1)/3B_m - \rho r/3B_m + \{\,(\sigma_y)_m \nu_m / E_m\,\} \cdot (r_d^3/r^2) - \alpha_m \cdot r \cdot \Delta T \qquad (40)$$

Knowing the displacement u, the strain components in the plastic zone ($r_1 \le r \le r_d$) can be determined as follows.

$$(\epsilon_r)_m = -du/dr = \{\,2(\sigma_y)_m/3B_m\,\} \cdot \{\,\ln(r/r_1) + 1\,\} - \rho/3B_m - \{\,2(\sigma_y)_m \cdot \nu_m/E_m\,\} \cdot (r_d/r)^3 - \alpha_m \Delta T \qquad (41)$$

$$(\epsilon_\theta)_m = -u/r = \{\,2(\sigma_y)_m/3B_m\,\} \cdot (\ln(r/r_1) - \rho/3B_m - \{\,(\sigma_y)_m \nu_m/E_m\,\} \cdot (r_d/r)^3 - \alpha_m \Delta T \qquad (42)$$

Employing the stress-strain relations, given by Equations (35) and (36), the yield condition $(\sigma_y)_m = (\sigma_\theta)_m - (\sigma_r)_m$, and the incompressibility condition $(\epsilon_r)_m^p = -2(\epsilon_\theta)_m^p$, the plastic strain components are determined as

$$(e_r)_m^p = -2(e_\theta)_m^p = \{ 2(\sigma_y)_m/E_m \} \cdot [1 - \nu_m \{ 1 + (r_d/r)^3 \}] \tag{43}$$

The elastic strain components, $(\epsilon_r)_m^e$ and $(\epsilon_\theta)_m^e$ are obtained by subtracting the plastic strain components, Equation (43), from the total strains, Equations (41) and (42).

$$\begin{aligned}(e_r)_m^e &= (e_r)_m - (e_r)_m^p \\ &= (1/3B_m) \cdot \{ 2(\sigma_y)_m \cdot \ln(r/r_1) - \rho \} - 2(\sigma_y)_m \nu_m/E_m \\ &\quad - \alpha_m \Delta T\end{aligned} \tag{44}$$

$$\begin{aligned}(e_\theta)_m^e &= (e_\theta)_m - (e_\theta)_m^p \\ &= (1/3B_m) \cdot \{ 2(\sigma_y)_m \cdot \ln(r/r_1) - \rho \} - \{ (\sigma_y)_m/E_m) \cdot (1 - \nu_m) \} \\ &\quad - \alpha_m \Delta T\end{aligned} \tag{45}$$

THERMAL FATIGUE LIFE

On the basis of Manson's (13) and Garmong's (14) reports on the applicability of the low cycle fatigue damage model to the thermal fatigue, the Coffin-Manson relationship (12, 13) can be utilized for the estimation of thermal fatigue life.

$$(\epsilon)^p = M.N_f^z \tag{46}$$

where

$(\epsilon)^p$: plastic strain per thermal cycle

M, z : material constants

N_f : number of thermal cycles at failure.

With total strain, Manson's simplified equation (37) may be employed.

$$(\epsilon) = 3.5 \cdot (\sigma_u/E) \cdot (N_f)^{-0.12} + (\epsilon_f)^{0.6} \cdot (N_f)^{-0.6} \quad (47)$$

where

(ϵ) : total strain per thermal cycle = $(\epsilon)^e + (\epsilon)^p$

σ_u : ultimate strength

(ϵ_f) : true fracture strain in a monotonic tensile test

CONCLUSIONS

1. In a MMC with a spherical reinforcement particle, the CTE mismatch-induced thermoelastic stresses and strains are largest at the reinforcement particle/matrix interface, and they decrease with distance from the interface.

2. The spherical reinforcement particle is in a state of hydrostatic stress, which is larger with larger elastic modulus, CTE, and temperature range.

3. Plastic deformation starts in the matrix adjacent to the reinforcement particle. Consequently, the interface is a potential site for crack initiation under thermal cycling.

4. The critical internal pressure for plastic deformation is less than 2/3 of the yield stress of a given matrix material, and it decreases with increasing range of temperature fall.

5. With the analytically determined strain, the thermal fatigue life can be estimated by employing the Coffin-Manson relationship.

REFERENCES

1. S. Yoda, N. Kurihara, K. Wakashima, and S. Umekawa, Metall. Trans., 9A, (1978), 1229-1236.

2. S. Yoda, N. Kurihara, K. Wakashima, and S. Umekawa, Metall. Trans., 10A, (1979), 1796-1798.

3. D. W. Petrasek and R.A. Signorelli, Eng. Sci, Proc., 7 & 8, (1981), 739-786.

4. H.H. Grimes, R.A. Lad, and J.E. Maisel, Metall, Trans., 8A, (1977), 1999 ^005.

5. G.C. Olsen and S.S. Thompkins, Failure Modes in Composites, IV, Edited by J.A. Cornie and F.W. Crossman, TMS of AIME, (1977), 1-21.

6. M.A. Wright, Metall, Trans., 6A, (1975), 129-134.

7. W.H. Kim, M. J. Koczak, and A. Lawley, New Developments and Applications in Composites, Edited by D. Kuhlmann-Wilsdorf and W.C. Harrigan, Jr., TMS of AIME, (1979), 40-53.

8. R.T. Bhatt and H.H. Grimes, Mechanical Behavior of Metal-Matrix Composites, Edited by J.E. Hack and M.F. Amateaux, TMS of AIME, (1983), 51-64.

9. Y.H. Park and H.L. Marcus, ibid., 65-75.

10. W.G. Patterson and M. Taya, Proc. ICCM-V, Edited by W.C. Harrigan, Jr. et al., TMS of AIME, (1985), 53-66.

REFERENCES (Continued)

11. T. Kyono, I.W. Hall, and M. Taya, Composites '86: Recent Advances in Japan and the United States, Edited by K. Kawata et al., Japan Society for Composite Materials, (1986), 553-561.

12. L.F. Coffin, Jr., Trans. ASME, 76, (1954), 923-949.

13. S.S. Manson, Thermal Stress and Low-Cycle Fatigue, McGraw-Hill Book Co., (1966), 88-89, 132-134, 245-274.

14. G. Garmong, Metall, Trans., 5, (1974), 2199-2205.

15. D.A. Koss and S. M. Copley, Metall, Trans., 2, (1971), 1557-1560.

16. F. Laszlo, J. Iron Steel Inst., 148, (1943), 173-199.

17. S.S. Hecker, S.S. Hamilton, and L.J. Ebert, J. Mater., 5, (1970), 868-900.

18. D. Iesan, J. Thermal Stress, 3, (1980), 495-508.

19. R.M. Christensen and H. Lo, J. Mech. Phys. Solids, 27, (1979), 315-330.

20. Y. Mikata and M. Taya, J. Comp. Mater., 19, (1985), 554-578.

21. G.J. Dvorak, J. Appl. Mech., 53, (1986), 737-743.

REFERENCES (Continued)

22. B.K. Min, J. Mech. Phys. Solids, 29, (1981), 327-352.

23. B.K. Min and F.W. Crossman, Composite Materials: Testing and Design, ASTM STP 788, Edited by I.M. Daniel, American Society for Testing and Materials, Philadelphia, PA (1982), 371-392.

24. S.D. Tsai, D. Mahulikar, H.L. Marcus, I.C. Noyan, and J.B. Cohen, Mater, Sci. Eng., 47, (1981), 145-149.

25. R.J. Arsenault and M. Taya, Proc. 4th Int. Conf. on Compostite Materials, San Diego, CA, July 1985.

26. Y. Bahei-El-Din and G.J. Dvorak, J. Appl. Mech., 49, (1982), 740-746.

27. C.C. Chamis, J. Reinforced Plastics and Composites, 6, (1987), 268-28.

28. J. Aboudi, Int. J. Plasticity, 4, (1988), 103-125.

29. J.L. Teply and G.J. Dvorak, J. Mech. Phys. Solids, 6, (1988), 29-58.

30. Y. Mikata and M. Taya, J. Comp. Mater., 19, (1985), 554-578.

31. A.L. Highsmith, D. Shin, and R.A. Naik, Thermal and Mechanical Behavior of Metal Matrix and Ceramic Matrix Composites, ASTM STP 1080, Edited by J.M. Kennedy, H.H. Moeller, and W. S. Johnson, American Society for Testing and Materials, Philadelphia, PA, (1990), 3-19.

REFERENCES (Continued)

32. R.J. Arsenault and M. Taya, Acta Metal., 35, (1987), 651-659.

33. G.S. Daehn, Thermal and Mechanical Behavior of Metal Matrix and Ceramic Matrix Composites, ASTM STP 1080, Edited by J.M. Kennedy, H.H. Moeller, and W. S. Johnson, American Society for Testing and Materials, Philadelphia, PA, (1990), 70-86.

34. H.H. Ledbetter and M.W. Austin, Mater. Sci. Eng., 89, (1989), 53-61.

35. Y.K. Klipfel, M.Y. He, R.M. McMeeking, A.G. Evans, and R. Mehrabian, Acta Metal., 38, (1990), 1063-1074.

36. G.E. Dieter, Mechanical Metallurgy, McGraw-Hill Book Co., New York, N.Y., 1961, 62.

37. S.S. Manson, Exp. Mech., 5, (1965), 193-226.

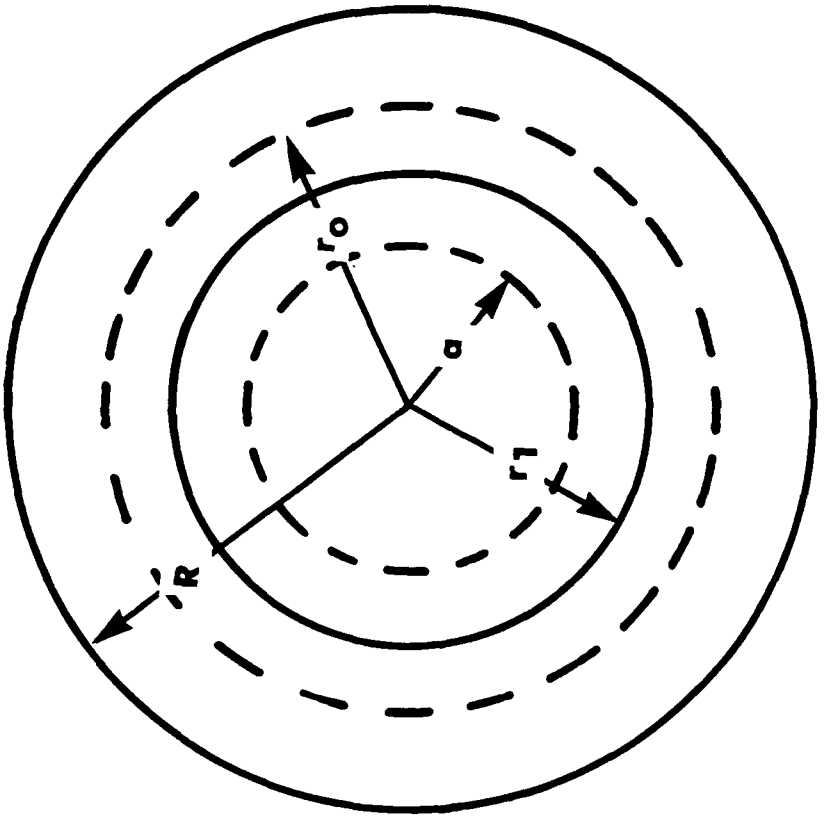

Figure 1. Schematic of Spherical Reinforcement Particle and Matrix Hole.

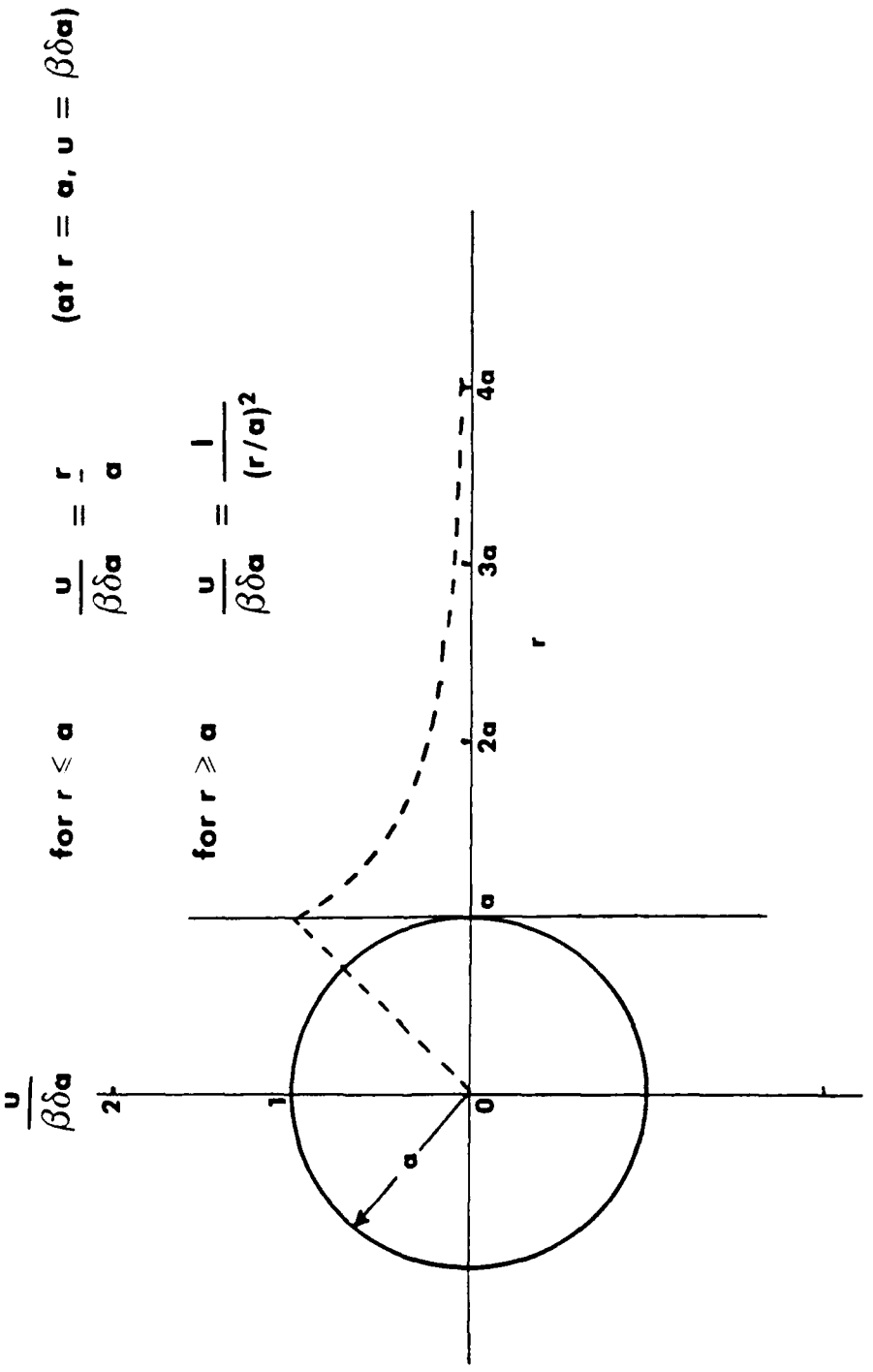

Figure 2. Elastic Strain Component Variation with Radial Distance.

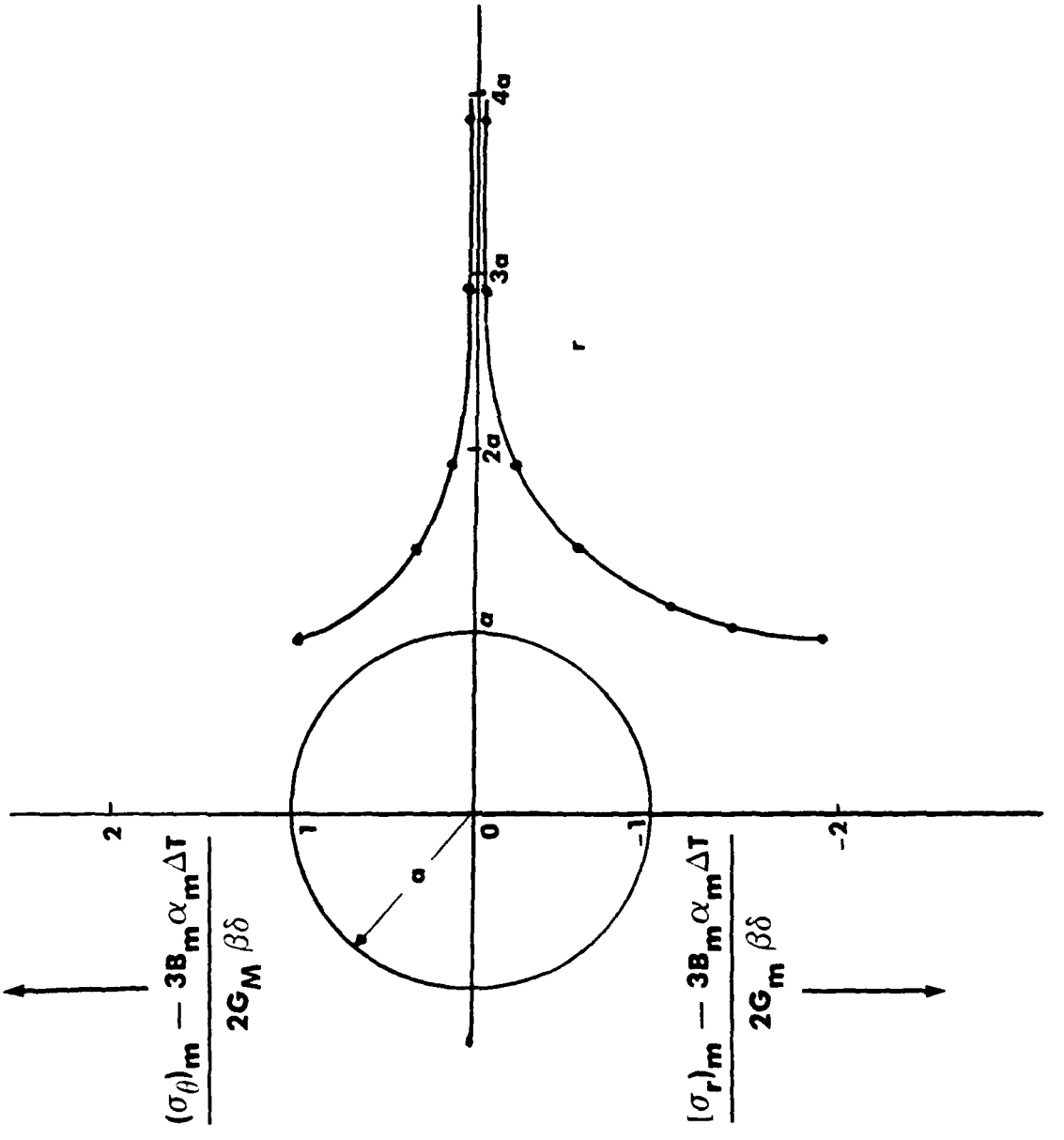

Figure 3. Elastic Stress Component Variation with Radial Distance.

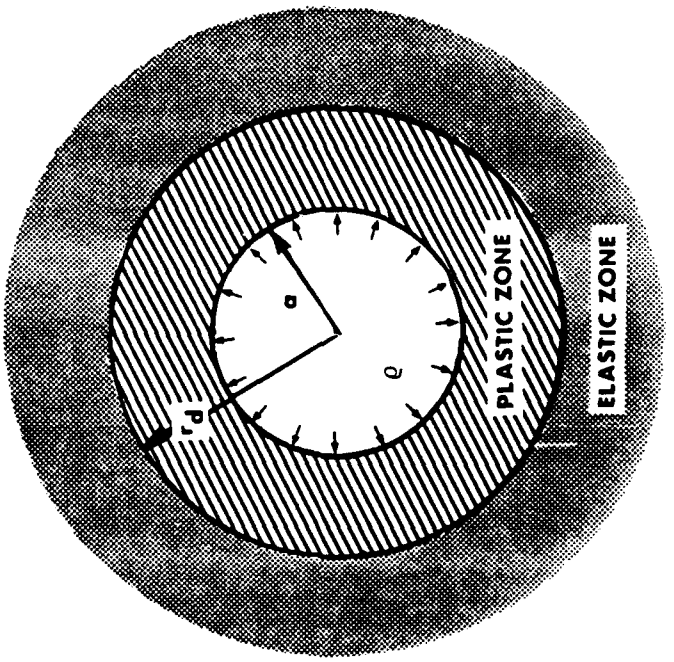

Figure 4. Thick Hollow Sphere Under Internal Pressure.

DISTRIBUTION LIST (Continued)
Report No. NADC-91059-60

	No. of Copies
Naval Air Development Center Warminster, PA 18974-5000 (20 for Code 6063) (2 for Code 8133)	22
Annapolis Laboratory David W. Taylor Naval Ship Research and Development Center Detachment Annapolis, MD 21402-1198	1
Naval Aviation Depot Naval Air Station Code 340 Alameda, CA 94501-5201	1
Naval Aviation Depot Marine Corps Air Station Code 340 Cherry Point, NC 28533-5030	1
Naval Aviation Depot Naval Air Station Code 340 Jacksonville, FL 32212	1
Naval Aviation Depot Naval Air Station Code 340 Norfolk, VA 23511-5899	1
Naval Aviation Depot ~~North Island~~ Code 340 Pensacola, FL 32508-5300	1
Naval Aviation Depot Naval Air Station Code 340 San Diego, CA 92135-5112	1
Naval Post Graduate School Monterey, CA 93940 Attn: Dr. E. R. Wood (Code 67)	1

DISTRIBUTION LIST
Report No. NADC-91059-60

	No. of Copies
Naval Air Systems Command Washington, DC 20361-3030 (2 for AIR-530) (2 for AIR 931A) (1 for AIR-5302) (1 for AIR-5304)	6
Naval Sea Systems Command Washington, DC 20362	1
Naval Safety Center NAS, Norfolk, VA 23511	1
Naval Air Test Center Patuxent River, Md 20670-5304	1
Naval Research Laboratory 4555 Overlook Ave., SW Washington, DC 20375	1
David W. Taylor Naval Ship Research and Development Center Bethesda, MD 20084-5000	1
U.S. Air Force Systems Command Wright-Patterson AFB, OH 45433 (1 for FBR) (1 for FB) (1 for LLD) (1 for FYA) (1 for LAM) (1 for FBA) (1 for LPH)	7
Chief of Naval Research 800 N. Quincy St. Arlington, Va 22217-5000	1
Defense Technical Information Center ATTN: DTIC-FDAB Cameron Station BG5 Alexandria, VA 22304-6145	2
Center for Naval Analysis 4401 Fort Avenue P.O. Box 16268 Alexandria, VA 22302-0268	1